Inhibition of DNA Binding by Human Estrogen-Related Receptor 2 and Estrogen Receptor α with Minor Groove Binding Polyamides†

Micah D. Gearhart,‡ Liliane Dickinson,‡ Jennifer Ehley,‡ Christian Melander,‡,§ Peter B. Dervan,§ Peter E. Wright,‡ and Joel M. Gottesfeld*,‡

Department of Molecular Biology, The Scripps Research Institute, La Jolla, California 92037, and Division of Chemistry and Chemical Engineering, California Institute of Technology, Pasadena, California 91125

Received October 1, 2004; Revised Manuscript Received January 13, 2005

ABSTRACT: Human estrogen-related receptor 2 (hERR2, ESRRB, ERRβ, NR3B2) belongs to a class of nuclear receptors that bind DNA through sequence-specific interactions with a 5′-AGGTCA-3′ estrogen response element (ERE) half-site in the major groove and an upstream 5′-TNA-3′ site in the minor groove. This minor groove interaction is mediated by a C-terminal extension (CTE) of the DNA binding domain and is unique to the estrogen-related receptors. We have used synthetic pyrrole−imidazole polyamides, which bind specific sequences in the minor groove, to demonstrate that DNA binding by hERR2 is sensitive to the presence of polyamides in both the upstream minor groove CTE site and the minor groove of the ERE half-site. Thus, polyamides can inhibit hERR2 by two mechanisms, by direct steric blockage of minor groove DNA contacts mediated by the CTE and by changing the helical geometry of DNA such that major groove interactions are weakened. To confirm the generality of the latter approach, we show that the dimeric human estrogen receptor α (hERα, ESR1, NR3A1), which binds in the major groove of the ERE, can be inhibited by a polyamide bound in the opposing minor groove of the ERE. These results highlight two mechanisms for inhibition of protein−DNA interactions and extend the repertoire of DNA recognition motifs that can be inhibited by polyamides. These molecules may thus be useful for controlling expression of hERR2- or hERα-responsive genes.

The human estrogen-related receptor 2 (hERR2,[1] ESRRB, ERRβ, NR3B2) is an orphan nuclear receptor protein that contains an N-terminal DNA binding domain (DBD) and a C-terminal ligand binding domain (*1*). hERR2 belongs to a unique subset of nuclear receptors that bind as monomers to extended estrogen response element (ERE) half-site DNA sequences with high affinity (*2*). Structural studies have confirmed that the hERR2 monomer makes sequence-specific contacts in both the major and minor grooves (*3*). The core 66 amino acids of the hERR2 DBD are similar to the human estrogen receptor (hERα, ESR1, NR3A1) and like hERα bind to a six base pair (bp) ERE half-site in the major groove (Figure 1). In contrast to hERα, which binds as a homodimer (Figure 1A) and makes sequence-specific contacts exclusively in the major groove (*4*), a C-terminal extension (CTE) immediately following the hERR2 DBD traverses the phosphate backbone and makes base-specific contacts with a three bp sequence in the minor groove 5′ (upstream) of the half-site (Figure 1B). C-Terminal to the residues that make minor groove contacts, the polypeptide chain exits the minor groove and makes DNA-induced intramolecular interactions with a region of the core DBD that can be used as an intermolecular interface in a heterodimeric nuclear receptor complex such as TR/RXR (*5*). The minor groove contacts and DNA-induced intramolecular packing are both critical components of the monomeric binding mechanism used by the hERR2 class of nuclear receptor proteins.

To investigate the contributions of the major and minor groove interactions toward the overall binding affinity of hERR2, synthetic DNA ligands were used to indirectly disfavor major groove interactions in the half-site and directly preclude the CTE binding in the 5′ extension to the half-site (Figure 1C). Hairpin polyamides are pyrrole (Py) and imidazole (Im) synthetic oligomers that bind in the minor groove of DNA with high specificity and affinity (reviewed in ref *6*). An Im/Py pair and a Py/Im pair target a G·C bp and a C·G bp, respectively, while a Py/Py pair binds to either an A·T or a T·A bp. Previous studies have shown that these ligands inhibit the DNA binding activities of proteins that bind in both the minor groove (*7*−*10*) and the major groove (*11*−*14*) of DNA by allosteric inhibition.

This study was designed to extend the repertoire of allosteric inhibition by polyamides to the nuclear receptor class of DNA binding domains. By comparing the inhibitive properties of polyamides to major groove binding by ERα with the major and minor groove binding features of hERR2, we contrast the direct and indirect mechanisms of polyamide inhibition. We also examine the relationship between the

† This work was supported by National Institutes of Health Grants CA84192 (to J.M.G.), GM57148 (to J.M.G. and P.B.D.), and GM36643 (to P.E.W.).

* To whom correspondence should be addressed. Telephone: 858-784-8913. Fax: 858-784-8965. E-mail: joelg@scripps.edu.

‡ The Scripps Research Institute.

§ California Institute of Technology.

[1] Abbreviations: hERR2, human estrogen-related receptor 2; hERα, human estrogen receptor α; DBD, DNA binding domain; ERE, estrogen response element; CTE, C-terminal extension; bp, base pair; EMSA, electrophoretic mobility shift assay; Py, *N*-methylpyrrole; Im, *N*-methylimidazole.

10.1021/bi047872o CCC: $30.25
Published on Web 02/26/2005

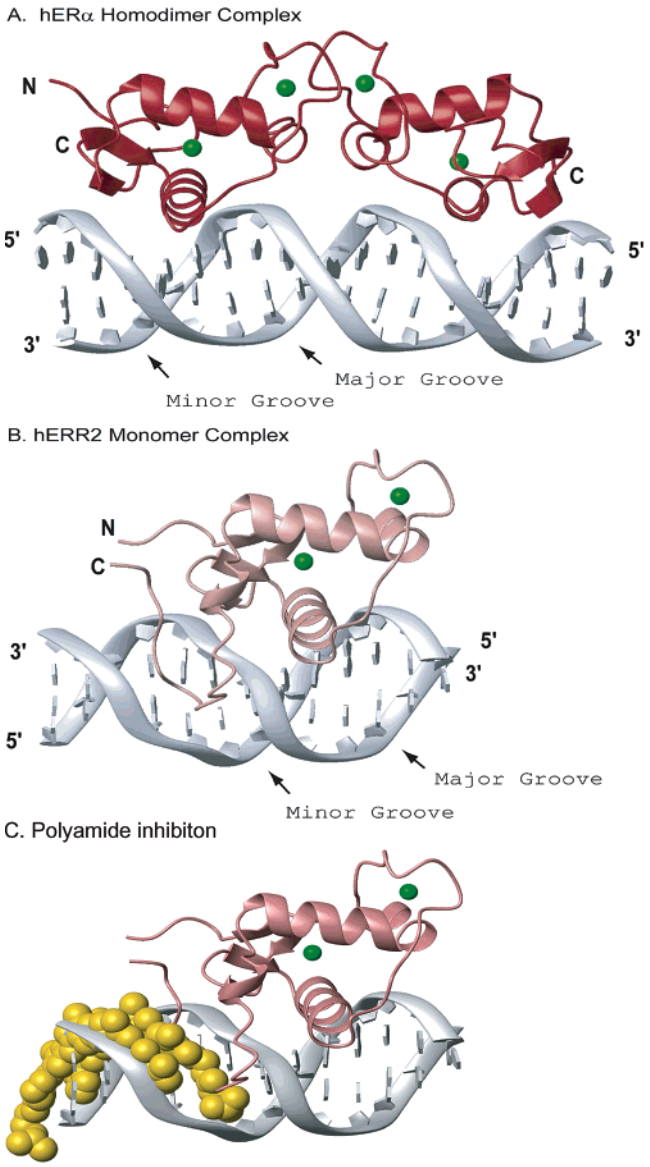

FIGURE 1: Structural comparison of DNA binding by hERα and hERR2. (A) The crystal structure of the hERα homodimer bound to the estrogen response element (ERE) inverted repeat duplex sequence, 5′-CCAGGTCACAGTGACCTG-3′ [1HCQ (*4*)]. (B) The solution structure of monomeric hERR2 bound to an extended half-site duplex sequence, 5′-GCTCAAGGTCAGC-3′ [1LO1 (*3*)]. The topology of the core DBD is similar for hERα and hERR2 in the recognition of the 5′-AGGTCA-3′ half-site in the major groove. hERR2 makes additional sequence-specific contacts in the minor groove upstream of the half-site by using a AT-hook-like motif appended to the core DBD. Schematic representations of the protein backbone, zinc atoms, and DNA sequences were created using MOLMOL. (C) Model for the steric blockage of the hERR2 CTE by a polyamide located in the minor groove.

location of the polyamide binding site and inhibition of protein binding by the indirect mechanism. We find that polyamides that target the minor groove interaction mediated by the CTE are strong direct inhibitors of hERR2 binding. Major groove interactions mediated by either hERR2 or hERα can be inhibited by polyamides occupying the opposing minor groove of the ERE.

MATERIALS AND METHODS

Polyamide Synthesis. Polyamides **1**−**3** were synthesized, purified, and confirmed as described in ref *15*. Structures of ImPyPyPy-γ-ImPyPyPy-β-Dp (**1**), ImPyImPy-γ-PyPyPyPy-β-Dp (**2**), and ImImPyPy-γ-ImPyPyPy-β-Dp (**3**) (where Im = imidazole, Py = pyrrole, β = β-alanine, γ = γ-aminobutyric acid, and Dp = dimethylaminopropylamide) are shown in Figure 2A along with binding models.

Protein Expression and Purification. The hERR2 C163A DBD was expressed, purified, and refolded as described previously by substituting unlabeled ammonium sulfate [$(NH_4)_2SO_4$] and glucose in the minimal media (*16*). The identity and integrity of purified protein were confirmed by mass spectrometry. Protein concentrations were determined using UV spectroscopy (*17*). Full-length human ERα was purchased from PanVera (Madison, WI).

Gel Shift Assays. The oligonucleotides shown in Figure 2B,C were synthesized (Genosys Biotechnologies, Inc.) for use as double-stranded probes in the gel shift assays for hERR2 binding and inhibition experiments. The probes contain 5′ overhangs (5′-TCGA-3′) for subsequent cloning. Oligonucleotides were labeled with T4 polynucleotide kinase (New England Biolabs) using [γ-^{32}P]ATP (NEN Life Sciences). The complementary strands were combined and annealed by heating to 95 °C and slowly cooled. Annealed, double-stranded oligonucleotides were purified on a nondenaturing 15% polyacrylamide gel in TBE buffer [0.089 M Tris−borate, 0.002 M EDTA (ethylenediaminetetraacetic acid), pH 8.3] at 250 V for 2 h. Oligonucleotides were allowed to diffuse out of excised bands and passed over an Elutip-D Cartridge (Schleicher & Schuell). DNA was precipitated in the presence of 20 μg of glycogen from the high-salt eluent and resuspended in 50 μL of 100 mM Tris-HCl, pH 8.0, and 20 mM KCl. For hERα binding experiments, the oligonucleotides had the following sequences: top strand, 5′-GATCCAAAGTCAGGTCACAGTCACCTGATCAAAGA-3′, and bottom strand, 5′-GATCTCTTTGATCAGGTCACTGTGACCTGACTTTG-3′, and were annealed as above and end labeled with [α-^{32}P]dATP (NEN Life Sciences) using the Klenow fragment of DNA polymerase (Roche Molecular Biosciences). Binding reactions, containing approximately 1.8 nM labeled DNA probe, 25 mM Tris-HCl, pH 8.0, 1 mM DTT, 50 mM KCl, 0.05 mg/mL poly(dI-dC) (Amersham Biosciences), 2.5 mg/mL bovine serum albumin, 0.1% (v/v) Igapal CA-630 (Sigma, previously known as NP-40), and 10% (v/v) glycerol, were incubated with varying concentrations of protein for 20 min before being loaded on a 10% nondenaturing polyacrylamide gel in TB buffer (0.089 M Tris−borate, pH 8.3) and run at 100 V for 45 min. Gels were dried and exposed to a Kodak phosphorimaging screen overnight. A Molecular Dynamics PhosphorImager SI was used to create a digital image of the gel. Band intensities were quantitated using the ImageQuant 1.2 software package from Molecular Dynamics. The fraction of DNA bound was calculated as the intensity of the shifted band over the sum of the intensities of the shifted and unshifted bands. Apparent dissociation contacts were calculated by fitting the fraction of DNA bound versus protein concentration with the Hill equation, using fixed Hill coefficients of 1.0, with the software package Kaleidagraph (Synergy Software).

DNase I Footprinting. The oligonucleotides shown in Figure 2B,C were annealed, phosphorylated with T4 polynucleotide kinase and unlabeled ATP, and cloned into pBluescript II KS(+) phagemid DNA (Stratagene), previ-

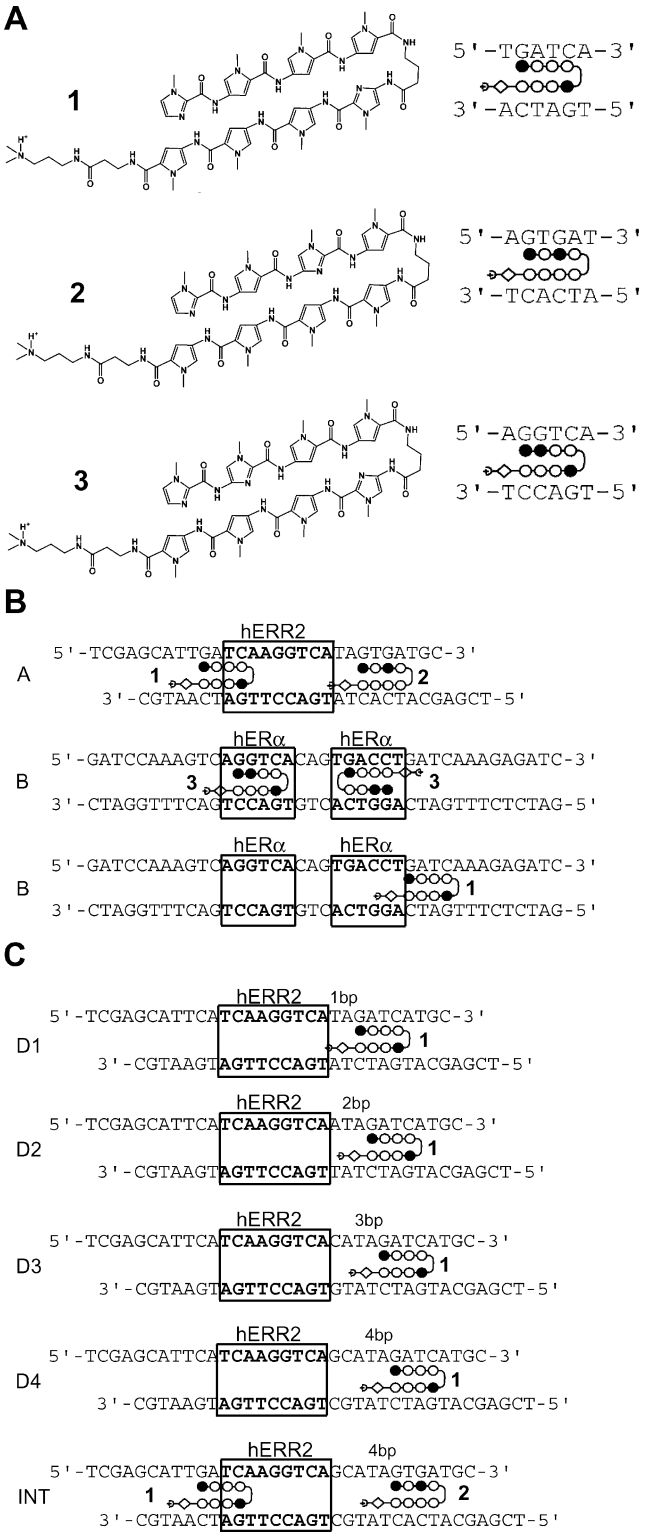

FIGURE 2: Polyamide structures, oligonucleotides, and binding models. (A) Structures of ImPyPyPy-γ-ImPyPyPy-β-Dp (**1**), ImPyImPy-γ-PyPyPyPy-β-Dp (**2**), and ImImPyPy-γ-ImPyPyPy-β-Dp (**3**), where Im = imidazole, Py = pyrrole, β = β-alanine, γ = γ-aminobutyric acid, and Dp = dimethylaminopropylamide. (B, C) Oligonucleotide sequences contain the hERR2 and hERα recognition elements (boxed regions) and polyamide binding sites. Binding models for each polyamide with matching DNA sites are shown. For oligonucleotide **B**, binding models for polyamides **1** and **3** are shown separately. The solid and open circles represent Im and Py rings, respectively, the hairpin junction formed with γ-aminobutyric acid is shown as a curved line, the diamond represents β-alanine, and a half-circle with plus sign represents Dp.

ously digested with the restriction enzyme *Xho*I. The identities of the clones were verified by DNA sequencing. A 328 base pair *Pvu*II/*Xba*I restriction fragment was end labeled with [α-^{32}P]ATP using the Klenow fragment of DNA polymerase (Roche Molecular Biosciences) and purified on a 10% nondenaturing TBE gel. The DNA fragments are labeled at the 3′ end of the bottom strand. G + A sequencing reactions were performed with formic acid and piperidine as described (*18*). Binding reactions were performed in a buffer identical to gel shift reactions with the omission of the nonspecific competitor. The reactions (100 μL) were supplemented with 2 mM $CaCl_2$ and 5 mM $MgCl_2$ prior to a 30 s digestion with DNase I (Roche Molecular Biosciences). Digestions were stopped by the addition of 110 μL of stop buffer (1.0% SDS, 0.5 M NaCl, 50 mM Tris-HCl, pH 7.6, and 25 mM EDTA), extracted with phenol/chloroform, and precipitated with ethanol using glycogen (20 μg) as a carrier. Samples were denatured by heating to 95 °C for 5 min in 95% formamide and electrophoresed on a 6% denaturing polyacrylamide gel, containing 7.6 M urea, 0.089 M Tris−borate, pH 8.3, and 2 mM EDTA. Gels were dried and exposed to Kodak Biomax film at ambient temperature or storage phosphorimage screens. The extent of protection was determined by phosphorimage analysis and ImageQuant software, using appropriate background correction. The intensity of a set of bands within the protein or polyamide footprint was normalized to a set of bands outside of the footprint to correct for differences in loading and extents of DNase digestion between lanes.

RESULTS AND DISCUSSION

An oligonucleotide probe was designed with polyamide binding sites at two locations with respect to the hERR2 consensus recognition element (Figure 2B). Oligonucleotide **A** contains a binding site for polyamide **1** immediately 5′ of the 5′-AGGTCA-3′ half-site and was designed such that polyamide binding at this site would directly conflict with minor groove contacts to 5′-TCA-3′ made by residues in the CTE of hERR2 (modeled in Figure 1C). Additionally, a binding site for polyamide **2** was engineered into oligonucleotide **A** one bp 3′ of the ERE half-site, in close vicinity to the major groove binding region of hERR2. Polyamide binding at this site has the potential to alter the geometry of the DNA and slightly compress the major groove (see below). Therefore, the design of oligonucleotide **A** facilitates the use of two isomeric polyamides to inhibit hERR2 binding by two distinct mechanisms. In previous quantitative footprinting experiments under equilibrium conditions, polyamide **1** binds its target site with an apparent dissociation constant (K_d) of 30 pM (*19*), while polyamide **2** binds with a K_d of 0.6−1.4 nM (*10, 20*).

To demonstrate that polyamides bind the targeted sequences in oligonucleotide **A** and are able to inhibit hERR2 binding to the consensus recognition element, oliogonucleotide **A** was cloned in pBluescript, and a radiolabeled 328 bp restriction fragment containing the oligonucleotide **A** sequence was derived for footprinting experiments. hERR2 binds this DNA with a K_d of approximately 7 nM (Figure 3, lanes 8−11, and other footprinting experiments, not shown). Polyamides **1** and **2** also protect this fragment from DNase I cleavage in the regions including and surrounding their respective target sequences (Figure 3). Higher DNA con-

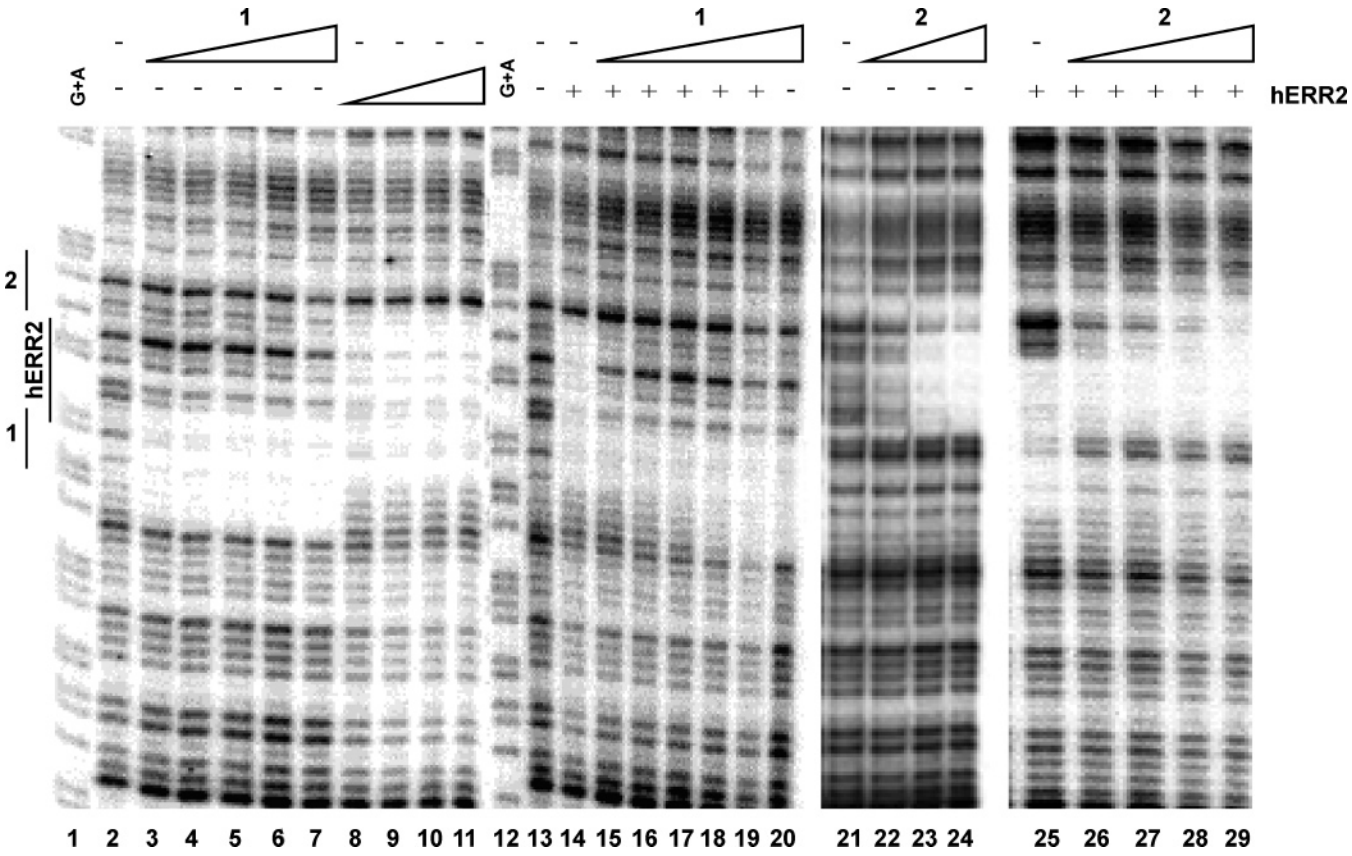

FIGURE 3: Polyamides **1** and **2** inhibit DNA binding by hERR2 in DNase I footprinting experiments. Lanes 1 and 12 depict formic acid G + A sequencing reactions of the 3′-end-labeled DNA (*18*); lanes 2, 13, and 21 show the products of DNase I digestion in the absence of polyamide or hERR2. Lanes 3−7 and 15−19 contained the following concentrations of polyamide **1**, 10, 25, 50, 100, and 200 nM, and lane 20 also contained 200 nM polyamide **1** (in the absence of hERR2). Lanes 8−11 contained the following concentrations of hERR2, 5, 20, 80, and 200 nM, respectively, and lanes 14−19 contained hERR2 at 200 nM. For polyamide **2** experiments, lanes 22−24 and 26−28 contained the following concentrations of polyamide, 10, 40, and 100 nM, respectively, and lane 29 contained 400 nM. Lanes 25−29 contained hERR2 at 150 nM. The location of polyamide and hERR2 binding sites is shown alongside the gels. Lanes 1−11, 12−20, 21−24, and 25−29, respectively, were taken from separate gels. The locations of polyamides **1** and **2** and hERR2 binding sites are shown alongside the phosphorimage of the footprinting gels.

centrations were used in the experiments depicted in Figure 3 than in previous footprinting experiments (*10*, *19*, *20*); thus higher polyamide concentrations are required for binding in the present experiments. Nonetheless, a polyamide **1** footprint is observed at a concentration of 10 nM on this DNA (Figure 3, lane 3). Polyamide **2** also binds its target site in this DNA fragment as evidenced by generation of a DNase I footprint (Figure 3, lanes 22−24). Note that the regions of DNase I protection afforded by hERR2 and both polyamides are larger than the respective binding sites for these ligands due to the steric properties of DNase I (*21*).

For hERR2 inhibition studies, the DNA fragment was incubated with increasing concentrations of polyamide **1** along with a saturating concentration (200 nM) of hERR2 (Figure 3, lanes 15−19). The hERR2 footprint, which is clearly visible in the absence of polyamide (lanes 8−11 and 14), disappears with increasing concentrations of polyamide **1** and is replaced by the polyamide footprint (lanes 15−19). The hERR2 footprint is clearly reduced by the lowest (10 nM) polyamide concentration tested. Thus, and as expected, polyamide **1** interferes with hERR2 binding at the upstream 5′-TCA-3′ site, where direct contacts are made with the minor groove. Similarly, polyamide **2** concentrations as low as 10 nM significantly inhibit DNA binding by hERR2 (Figure 3, lanes 26−29). These results suggest that polyamide binding at either the upstream 5′-TCA-3′ site or the downstream site weakens the binding of hERR2, and inhibition of hERR2 can be achieved by either direct steric blockage of the minor groove (at the upstream site) or an indirect mechanism at the downstream site.

To further investigate the indirect inhibition of major groove binding, DNase I footprinting experiments were used to ascertain the effect of the polyamide position relative to the half-site on hERR2 binding. Four additional oligonucleotides were designed (Figure 2C) containing polyamide **1** binding sites positioned between one and four base pairs downstream of the hERR2 binding site (D1−D4). A fifth oligonucleotide similar to oligonucleotide **A** with an internal binding site for polyamide **1** was used as a control (INT). Each of these oligonucleotides was cloned in pBluescript, and a radiolabeled 328 bp restriction fragment was isolated from each clone. DNase I footprinting experiments demonstrate that these sequence changes, both downstream and upstream from the ERE half-site, do not significantly affect either hERR2 or polyamide binding (Figure 4A and data not shown). Additionally, the footprinting experiments demonstrate that inhibition of hERR2 binding by the presence of polyamide **1** in the minor groove is dramatically reduced when the polyamide binding site is positioned two or more base pairs downstream from the hERR2 binding site. Cooccupancy of the DNA by both hERR2 and polyamide **1** is observed with the D2, D3, and D4 DNA probes (Figure 4A,

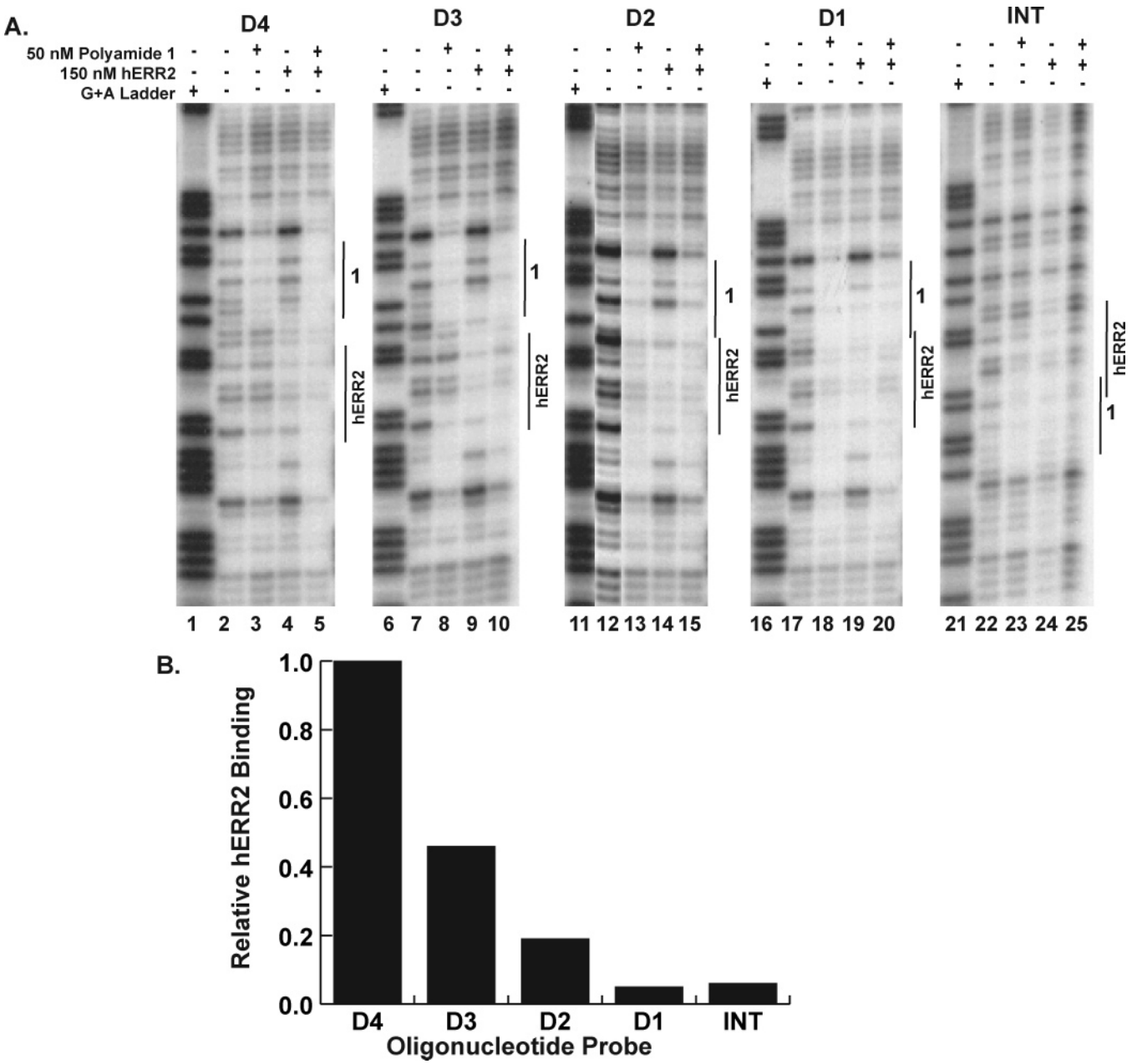

FIGURE 4: hERR2 binding is less inhibited as the polyamide binding site is moved downstream. (A) DNase I footprinting experiments using oligonucleotides D4, D3, D2, D1, and INT (as shown in Figure 2C) and polyamide **1**. Five reactions were performed for each oligonucleotide: a G + A sequencing reaction; DNA in the absence of either hERR2 or polyamide; 50 nM polyamide **1**; 150 nM hERR2; and 150 nM hERR2 with 50 nM polyamide **1**. The locations of polyamide and hERR2 binding sites for each DNA are shown alongside each gel. (B) Graphical representation of the results shown in panel A, where the relative binding of hERR2 in the presence of polyamide **1** is shown for each DNA construct. ImageQuant software was used to determine the fractional occupancy by hERR2 or polyamide in each reaction. Relative hERR2 binding was calculated as the ratio of intensity of the hERR2 footprint in the presence versus the absence of polyamide **1** for each oligonucleotide probe after gel loading and background corrections.

compare lanes 4 to 5, 9 to 10, and 14 to 15). In contrast, DNase I cleavage is observed within the hERR2 ERE for the D1 and INT probes in the presence of polyamide **1** (Figure 4A, compare lanes 19 to 20 and 24 to 25). Significantly, quantitative evaluation of DNase I footprint intensities shown in Figure 4B suggests that polyamide **1** was equally effective at inhibiting hERR2 binding in both the D1 and INT sequences. The ability of polyamide **1** to inhibit hERR2 binding is dramatically reduced as the polyamide **1** match site is moved further downstream in the D2, D3, and D4 sequences. Similar to the D4 probe, polyamide **2** fails to inhibit hERR2 binding to the INT probe (data not shown). These DNase I protection assays support the original observations that hERR2 binding is inhibited either by blocking direct minor groove contacts at the upstream site or by indirect effects on DNA geometry downstream of the hERR2 response element; however, the location of the polyamide binding site relative to the hERR2 response element is critical for inhibition to occur.

To ascertain the quantitative contributions of the major and minor groove interactions by hERR2, inhibition of hERR2 binding to oligonucleotide **A** by polyamides **1** and **2** was also monitored by electrophoretic mobility shift assays (EMSA). An example of a polyamide inhibition experiment is shown in Figure 5A. As polyamide **1** concentrations are increased, the amount of the hERR2−DNA complex (upper

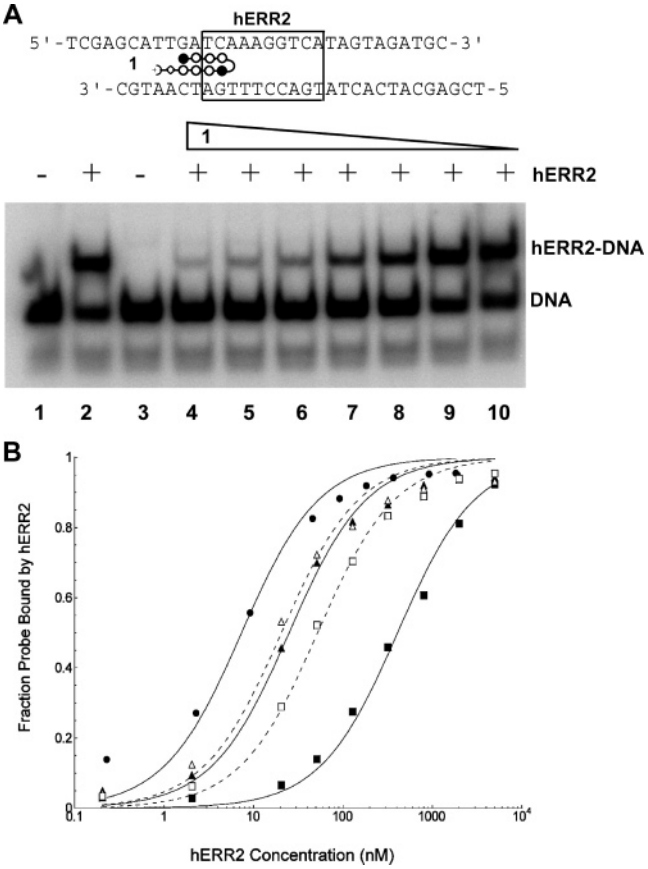

FIGURE 5: Polyamides **1** and **2** differentially inhibit hERR2 binding as assayed by EMSA. (A) EMSA phosphorimage of hERR2 binding to probe **A** (Figure 2B) in the absence or presence of polyamide **1**. Reactions contained hERR2 at a final concentration of 25 nM (where indicated by a plus sign) and increasing concentrations of polyamide **1** (200 nM, lanes 3 and 4; 100 nM, lane 5; 50 nM, lane 6; 25 nM, lane 7; 12.5 nM, lane 8; 6 nM, lane 9; 3 nM, lane 10). The positions of the free DNA and hERR2−DNA complex are indicated. (B) Effect of polyamides on the apparent dissociation constant for hERR2 binding to probe **A**, as determined by EMSA and phosphorimage analysis. Reactions contained increasing concentrations of hERR2 and either no polyamide (filled circles) or fixed concentrations of polyamides **1** or **2** (filled triangles, 50 nM **1**; filled squares, 500 nM **1**; open triangles, 50 nM **2**; open squares, 500 nM **2**). The lines represent nonlinear least-squares fits to the data obtained with Kaleidagraph software using the Hill equation, with a cooperativity parameter set to 1.0 for a simple bimolecular reaction. The K_d values are listed in Table 1.

band) is decreased and the amount of the uncomplexed DNA (lower band) increases. Note that the polyamide alone does not cause a change in mobility of the DNA (lane 3). Due to different assay conditions in the footprinting and EMSA experiments (higher DNA concentrations and the presence of nonspecific competitor DNA), higher polyamide concentrations are required to elicit inhibition in EMSA than in footprinting experiments. The ability of hERR2 to bind to oligonucleotide **A** is reduced to 50% of its original value by 20−50 nM polyamide **1**. EMSAs permit an accurate determination of the apparent dissociation constants for hERR2 binding in the presence of polyamide, thus permitting quantitative comparison between the effects of polyamides **1** and **2** on hERR2 binding. K_ds for hERR2 were determined by varying the protein concentrations at 0, 50, or 500 nM polyamides **1** or **2** (Figure 5B, Table 1). Significantly, similar K_d values for hERR2 binding to the oligonucleotide **A** sequence were obtained by EMSA and by DNase I footprinting (Figure 3). The K_ds for hERR2 at 0, 50, and 500 nM polyamide **1** are 7 ± 1, 25 ± 3, and 410 ± 30 nM, respectively (Table 1). The presence of polyamide **1** at 50 and 500 nM reduces the binding free energy of hERR2 for oligonucleotide **A** by +0.74 and +2.4 kcal/mol ($\Delta\Delta G$ values, Table 1), with respect to the binding of hERR2 in the absence of polyamide. The K_ds for hERR2 at 50 and 500 nM polyamide **2** are 21 ± 3 and 52 ± 4 nM, respectively, corresponding to $\Delta\Delta G$ values of +0.64 and +1.2 kcal/mol, with respect to the uninhibited interaction. The strong inhibition of hERR2 by polyamide **1** suggests that the minor groove contacts at the upstream site are more readily inhibited by polyamides.

Table 1: Effects of Polyamides **1** and **2** on hERR2 Binding Affinity

Polyamide	hERR2 binding affinity		ΔG	$\Delta\Delta G$
	K_d (nM)[a]	K_a (M^{-1})	(kcal/mol)[b]	(kcal/mol)[c]
none	7 ± 1	1.4×10^8	−11.04	0
1 (50 nM)	25 ± 3	4.0×10^7	−10.3	+0.74
1 (500 nM)	410 ± 30	2.4×10^6	−8.65	+2.39
2 (50 nM)	21 ± 3	4.8×10^7	−10.4	+0.64
2 (500 nM)	52 ± 4	1.9×10^7	−9.86	+1.18

[a] Determined by EMSA, as shown in Figure 5B. [b] Calculated from the equation $\Delta G = -RT(\ln K_a)$, where $T = 296$ K and R is 1.987. [c] Difference between the binding free energy of hERR2 in the presence and absence of the indicated concentration of polyamide.

To further investigate whether polyamide inhibition of nuclear hormone receptor binding at downstream sites is due to changes in DNA helix geometry, we monitored the effect of polyamide **3** (Figure 2A) on human estrogen receptor α (hERα) binding to a consensus oligonucleotide (Figures 2B and 6). hERα is a member of the nuclear hormone receptor superfamily of Cys_4 zinc finger transcription factors. These proteins recognize their cognate sequences through zinc finger-mediated base-specific contacts in the major groove of the ERE, and protein domains C-terminal to the zinc fingers make additional direct nonspecific contacts with the minor groove (*4*, *5*, *22*). EMSA experiments showed that recombinant hERα binds with high affinity to the sequence shown in Figure 6A (K_d = ∼2.5 nM; data not shown). Polyamide **3** is expected to bind within each ERE half-site (5′-AGGTCA-3′, Figure 6A), and such binding has been confirmed by DNase I footprinting, and a K_d of 1.0 nM was obtained in quantitative footprinting experiments (*11*). Consistent with the hERR2 results, polyamide **3** is an effective inhibitor of hERα binding, with 50% reduction in the amount of the input hERα−DNA complex at a polyamide concentration of ∼12.5 nM (Figure 6A). Order of addition experiments were performed to determine whether preincubation of the DNA with either hERα or the polyamide prior to addition of the other reaction component would have an effect on the polyamide concentration required for inhibition. Quantitation of such experiments showed that order of addition has only minimal effects (data not shown). The DNA sequence used for hERα binding studies contains a match site for polyamide **1** immediately downstream of the ERE (Figure 6B). In contrast to the results for polyamide **1** targeted to the half-site extension of the hERR2 binding site (Figure 5A), we find that this polyamide does not inhibit binding of hERα to this DNA, as assessed by EMSA (Figure 6B). Taken together, these results indicate that a minor

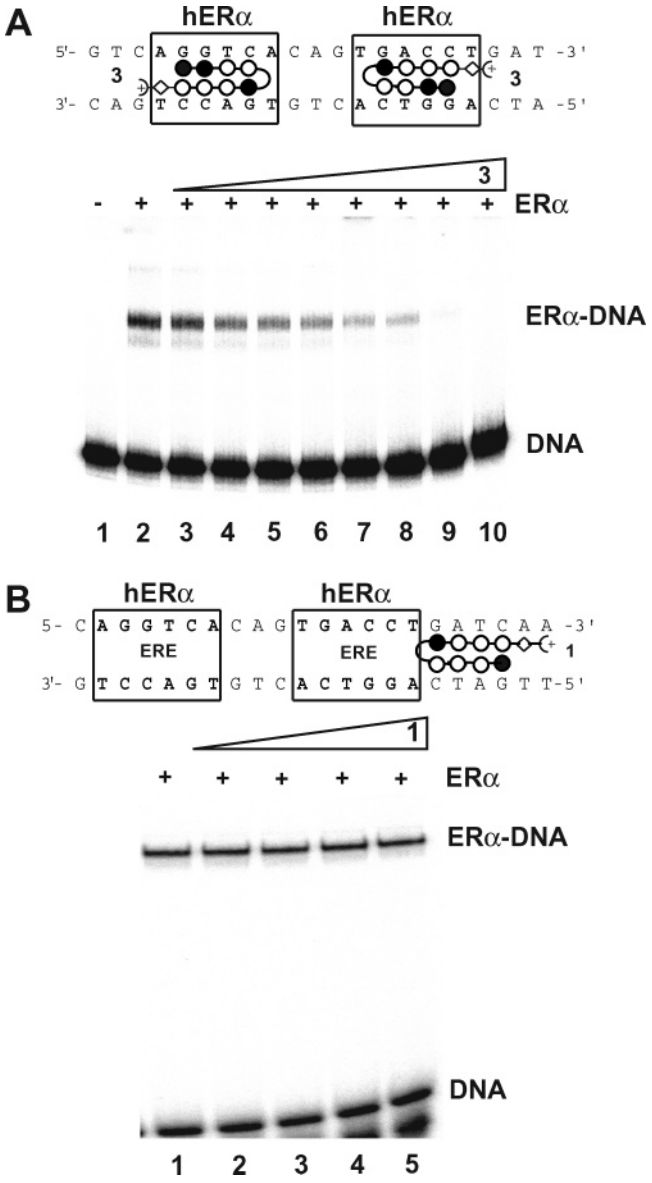

FIGURE 6: Polyamide inhibition of hERα binding. (A) DNA sequence used in gel mobility shift assays and a model for polyamide **3** binding within each ERE half-site, with symbols as in Figure 2B. EMSA for polyamide **3** inhibition of hERα binding: lane 1 contained the radiolabeled DNA alone; lanes 2−10 contained hERα at a final concentration of 2.5 nM, where 38% of the input DNA was bound by hERα in the absence of polyamide (as determined by phosphorimage analysis). In the reactions depicted in lanes 3−10, polyamide **3** was included at final concentrations of 3.1, 6.3, 12.5, 25, 50, 100, 200, and 400 nM, respectively. The positions of the free DNA and hERα−DNA complex are indicated. (B) Polyamide **1** located downstream of the ERE fails to inhibit hERα binding. A binding model for polyamide **1** is shown, where the match site is downstream of the ERE. Reactions contained hERα at a concentration of 2.5 nM and the following concentrations of polyamide **1**: no polyamide (lane 1); 25, 100, 200, and 400 nM in lanes 2−5, respectively. In the absence of polyamide, 42% of the input DNA is bound by hERα (lane 1). Different mobilities of the hERα−NA complex in panels A and B reflect different times of electrophoresis.

groove binding polyamide can inhibit the binding activity of the major groove binding nuclear hormone receptor hERα when the polyamide is located within the minor groove of the ERE. Additionally, targeting the minor groove outside of the 5′-AGGTCA-3′ half-site but within the 5′ extension recognized by hERR2 demonstrates that polyamide **1** can be used to selectively inhibit hERR2 binding.

Modeling studies were undertaken to assess potential mechanisms for inhibition of hERα binding. One possibility considered was that a polyamide bound in the minor groove might change the geometry of the DNA in the major groove such that hERα cannot bind simultaneously with the polyamide. Comparing the helical parameters between the crystal structures of ER DBD−DNA (*4*) and polyamide−DNA structures (*23*, *24*) indicates that the minor groove of polyamide-bound DNA is wider than that of ER-bound DNA; conversely, the major groove in the ER DBD−DNA structure is wider than that observed in polyamide−DNA structures. Groove widths differ between these two complexes most notably at the 5′-AGG-3′ portion of the ERE half-site. Thus, it is likely that these differences in groove geometries may be sufficient to diminish hERα binding affinity in the presence of polyamides. Another possible mechanism for inhibition of hERα binding is that the positively charged dimethylaminopropylamide tail of polyamide **3** interferes with DNA interactions made by the positively charged C-terminal linker region of hERα (K74), located between the zinc finger DNA binding domain and the ligand binding domain. This region of ER, which is important for DNA binding affinity, is directed toward the minor groove in the ER DBD−DNA crystal structure (*4*) and is located in the minor groove in structures of other nuclear receptor−DNA complexes (*5*, *22*). However, since polyamides placed downstream of the ERE half-site also inhibit hERR2 binding, we consider this latter possibility less likely than the allosteric mechanism. In this regard, inhibition of major groove-binding C_2H_2 zinc finger proteins with polyamides has been observed by this allosteric mechanism (*14*).

CONCLUSIONS

Minor groove binding polyamides targeted to either the upstream extension or a nonconserved region immediately downstream of the nuclear receptor half-site inhibit binding of hERR2 to the consensus recognition element. DNase I footprinting experiments demonstrate that polyamides can inhibit binding directly by blocking minor groove contacts and indirectly by altering DNA structure at extrinsic sites downstream of the hERR2 consensus binding site. Changes in DNA structure within approximately two base pairs sufficiently alter the structural properties of DNA and inhibit binding in the major groove. This type of allosteric inhibition is also observed with hERα, which binds as a dimer to an inverted repeat ERE in the major groove. A polyamide bound in the opposing minor groove was an effective inhibitor of hERα binding. Therefore, when targeting endogenous promoter sequences with polyamides, inhibition of transcription factor binding may be equally successful at sites proximal and internal to transcription factor binding sites. The hERR2 and hERα binding experiments support previous work that demonstrates that polyamides can be used to inhibit DNA binding by both minor and major groove binding proteins, by direct steric interference with minor groove binding proteins [such as TBP and LEF1 (*9*)], by steric interference with proteins that recognize their cognates sites in the major groove but make additional contacts either in or across the minor groove [such as the winged-helix protein Ets-1 (*11*), the zinc finger protein TFIIIA (*7*), and the basic helix−turn−helix protein Deadpan (*12*)], or by allosteric inhibition of

major groove binding proteins [such as C_2H_2 zinc finger proteins (*14*), NF-κB (*13*), and nuclear hormone receptors (this study)]. Allosteric inhibition is likely achieved by polyamide-induced changes in DNA helix geometry. We also probe the relationship between location of the polyamide binding site and inhibition of protein binding by the allosteric mechanism and find that the polyamide binding site must lie within two bp of the protein binding site for effective inhibition of protein binding. This distance is similar to that previously found for inhibition of TBP binding to the minor groove by polyamides (*25*).

ACKNOWLEDGMENT

We thank Dr. Clara Kielkopf for advice and assistance with modeling studies.

REFERENCES

1. Mangelsdorf, D. J., and Evans, R. M. (1995) The RXR heterodimers and orphan receptors, *Cell 83*, 841−850.
2. Sladek, R., Bader, J. A., and Giguere, V. (1997) The orphan nuclear receptor estrogen-related receptor alpha is a transcriptional regulator of the human medium-chain acyl coenzyme A dehydrogenase gene, *Mol. Cell. Biol. 17*, 5400−5409.
3. Gearhart, M. D., Holmbeck, S. M., Evans, R. M., Dyson, H. J., and Wright, P. E. (2003) Monomeric complex of human orphan estrogen related receptor-2 with DNA: a pseudo-dimer interface mediates extended half-site recognition, *J. Mol. Biol. 327*, 819−832.
4. Schwabe, J. W., Chapman, L., Finch, J. T., and Rhodes, D. (1993) The crystal structure of the estrogen receptor DNA-binding domain bound to DNA: how receptors discriminate between their response elements, *Cell 75*, 567−578.
5. Rastinejad, F., Perlmann, T., Evans, R. M., and Sigler, P. B. (1995) Structural determinants of nuclear receptor assembly on DNA direct repeats, *Nature 375*, 203−211.
6. Dervan, P. B., and Edelson, B. S. (2003) Recognition of the DNA minor groove by pyrrole-imidazole polyamides, *Curr. Opin. Struct. Biol. 13*, 284−299.
7. Neely, L., Trauger, J. W., Baird, E. E., Dervan, P. B., and Gottesfeld, J. M. (1997) Importance of minor groove binding zinc fingers within the transcription factor IIIA DNA complex, *J. Mol. Biol. 274*, 439−445.
8. Gottesfeld, J. M., Neely, L., Trauger, J. W., Baird, E. E., and Dervan, P. B. (1997) Regulation of gene expression by small molecules, *Nature 387*, 202−205.
9. Dickinson, L. A., Gulizia, R. J., Trauger, J. W., Baird, E. E., Mosier, D. E., Gottesfeld, J. M., and Dervan, P. B. (1998) Inhibition of RNA polymerase II transcription in human cells by synthetic DNA-binding ligands, *Proc. Natl. Acad. Sci. U.S.A. 95*, 12890−12895.
10. Dickinson, L. A., Trauger, J. W., Baird, E. E., Ghazal, P., Dervan, P. B., and Gottesfeld, J. M. (1999) Anti-repression of RNA polymerase II transcription by pyrrole-imidazole polyamides, *Biochemistry 38*, 10801−10807.
11. Dickinson, L. A., Trauger, J. W., Baird, E. E., Dervan, P. B., Graves, B. J., and Gottesfeld, J. M. (1999) Inhibition of Ets-1 DNA binding and ternary complex formation between Ets-1, NF-κB, and DNA by a designed DNA-binding ligand, *J. Biol. Chem. 274*, 12765−12773.
12. Winston, R. L., Ehley, J. A., Baird, E. E., Dervan, P. B., and Gottesfeld, J. M. (2000) Asymmetric DNA binding by a homodimeric bHLH protein, *Biochemistry 39*, 9092−9098.
13. Wurtz, N. R., Pomerantz, J. L., Baltimore, D., and Dervan, P. B. (2002) Inhibition of DNA binding by NF-kappa B with pyrrole-imidazole polyamides, *Biochemistry 41*, 7604−7609.
14. Nguyen-Hackley, D. H., Ramm, E., Taylor, C. M., Joung, J. K., Dervan, P. B., and Pabo, C. O. (2004) Allosteric inhibition of zinc-finger binding in the major groove of DNA by minor-groove binding ligands, *Biochemistry 43*, 3880−3890.
15. Baird, E. E., and Dervan, P. B. (1996) Solid-phase synthesis of polyamides containing imidazole and pyrrole amino acids, *J. Am. Chem. Soc. 118*, 6141−6146.
16. Sem, D. S., Casimiro, D. R., Kliewer, S. A., Provencal, J., Evans, R. M., and Wright, P. E. (1997) NMR spectroscopic studies of the DNA-binding domain of the monomer-binding nuclear orphan receptor, human estrogen related receptor-2. The carboxyl-terminal extension to the zinc-finger region is unstructured in the free form of the protein, *J Biol. Chem. 272*, 18038−18043.
17. Gill, S. C., and von Hippel, P. H. (1989) Calculation of protein extinction coefficients from amino acid sequence data, *Anal. Biochem. 182*, 319−326.
18. Maxam, A., and Gilbert, W. (1980) Sequencing end-labeled DNA with base-specific chemical cleavages, *Methods Enzymol. 65*, 497−559.
19. Trauger, J. W., Baird, E. E., and Dervan, P. B. (1996) Subnanomolar sequence-specific recognition in the minor groove of DNA by designed ligands, *Nature 382*, 559−561.
20. Gottesfeld, J. M., Melander, C., Suto, R. K., Raviol, H., Luger, K., and Dervan, P. B. (2001) Sequence-specific recognition of DNA in the nucleosome by pyrrole-imidazole polyamides, *J. Mol. Biol. 309*, 615−629.
21. Trauger, J. W., and Dervan, P. B. (2001) Footprinting methods for analysis of pyrrole-imidazole polyamide/DNA complexes, *Methods Enzymol. 340*, 450−466.
22. Zhao, Q., Khorasanizadeh, S., Miyoshi, Y., Lazar, M. A., and Rastinejad, F. (1998) Structural elements of an orphan nuclear receptor-DNA complex, *Mol. Cell 1*, 849−861.
23. Kielkopf, C. L., Baird, E. E., Dervan, P. B., and Rees, D. C. (1998) Structural basis for GC recognition in the DNA minor groove, *Nat. Struct. Biol. 5*, 104−109.
24. Suto, R. K., Edayathumangalam, R. S., White, C. L., Melander, C., Gottesfeld, J. M., Dervan, P. B., and Luger, K. (2003) Effects of ligand binding on structure and dynamics of the nucleosome core particle, *J. Mol. Biol. 326*, 371−380.
25. Ehley, J. A., Melander, C., Herman, D., Baird, E. E., Ferguson, H. A., Goodrich, J. A., Dervan, P. B., and Gottesfeld, J. M. (2002) Promoter scanning for transcription inhibition with DNA-binding polyamides, *Mol. Cell. Biol. 22*, 1723−1733.

BI047872O